Influence of Hydrodynamic Conditions and Water Chemistry on the Formation of Tufa in Huanglong, Sichuan

Liu Zaihua[1], Yuan Daoxian[1], W. Dreybrodt[2] and U. Svensson[2]

[1]Institute of Karst Geology, Guilin, China
[2]Institute of Experimental Physics, University of Bremen, Germany

Abstract

In order to study the origin of the local tufa deposits hydrochemical and hydrodynamic investigations have been carried out at a mainly spring-fed stream during two field campaigns. Preliminary results, supported by $\delta^{13}C$ data, suggest that calcite precipitation is entirely controlled by inorganic processes. The evolution of hydrochemistry with respect to major ions was measured at different locations downstream, whereby temperature, pH and specific conductance have been measured in situ. Small rectangular shaped tablets of pure marble were mounted in the stream-bed for an defined period of time and precipitation rates were measured from weight increase. Simultaneously, water samples were taken at the time of insertion and removal of the tablets. From the data of the water analysis the measured rates were compared to those calculated by the Plummer, Wigley and Parkhurst rate law. In general, the rates calculated by the PWP-rate law turned out to be too high, since these calculations do not consider the existence of a diffusion boundary layer of thickness ϵ, which is the major diffusive resistance between the calcite surface and the turbulently flowing solution. Application of a recently developed mass transfer model, which takes this effect into account displays, however, a distinct rate dependence on ϵ. The thickness of ϵ can be roughly estimated by hydrodynamic correlations, or can be measured in situ by gypsum samples of equal dimension as the marble tablets, mounted in close neighbourhood to the latter. Since dissolution of gypsum is entirely controlled by diffusion the thickness of ϵ can be estimated from weight loss. Furthermore, the hydrodynamic conditions, i.e. flow velocity should distinctly influence the value of ϵ and therefore calcite deposition rates. To verify this consideration the experiments have been performed under different hydrodynamic regimes of fast flowing water as well as under slow flow conditions. The measurements of calcite deposition rates by use of the experimentally determined values of ϵ between 0.005 to 0.01cm are in good correlation compared to those calculated theoretically.

1.Introduction

Inorganic precipitation of calcite from supersaturated spring and river water by degassing of CO_2 has been of considerable interest, both experimentally in the field and theoretically.

Since the first studies reported by Jacobson & Usdowski (1975) and Usdowski et al. (1979) an increasing amount of articles dealing with this topic

has been published (Suarez, 1983; Michaelis et al., 1984; Troester & White, 1986; Herman & Lorah, 1986; 1987; 1988). The precipitation rates reported have been obtained from mass balance considerations, which regard the calcium concentrations downstream. They have been compared to rates which have been calculated from the PWP-rate law, using the data of the chemical analysis of the stream water. In estimating, however, precipitation rates via mass balance one has to consider the lack of exact knowledge about important parameters, e.g. the surface area at which precipitation takes place or the exact flow velocity, which both are crucial to the conversion into experimentally observed rates. In a recently published paper Dreybrodt et al. (1992) have presented field experiments on calcite deposition in stream water, that have been performed by measuring both, hydrochemistry and precipitation rates simultaneously and comparing the obtained results directly. In applying the rate law of Plummer et al. (1978), however, one has to be careful since several restrictions have to be considered, given elsewhere (Plummer et al., 1978; 1979; Buhmann & Dreybrodt, 1985a,b; 1987).

In a subsequent paper Buhmann & Dreybrodt (1991) have extended their published results by a detailed investigation of turbulent flow effects. They take into account a diffusion boundary layer, which separates the solid from the turbulent bulk solution, where mass transport is determined by molecular diffusion. This boundary layer strongly reduces dissolution and precipitation rates by the occurrence of concentration gradients across it. With these extensions it is possible to predict dissolution and precipitation rates in turbulent flowing waters of natural chemical composition. A comprehensive review on the work cited above is given by Dreybrodt (1988). The present paper and the experimental field results are mainly based upon the theory given in the last mentioned paper (Buhmann & Dreybrodt, 1991). Furthermore, he intends to extend it to account for foreign ions as Mg^{2+}, Na^{+}, K^{+}, SO_4^{2-} and Cl^{-} (Buhmann & Dreybrodt, 1985b), which are always present in natural waters. Thus, we are able to calculate precipitation rates for actually measured compositions in a given stream.

2.1 *An Model of Mass Transfer*

Although the model is theoretically very complex, we will try to give some insight into the basic considerations, nevertheless strongly simplified. We assume that the liquid is divided into two regions. In a region adjacent to the solid surface a thin diffusion boundary layer of thickness δ exists, wherein mass transfer is entirely determined by molecular diffusion. Outside this layer one finds a turbulent and well mixed core, where eddy diffusity is so high, that a constant concentration C of all dissolved species can be assumed. Fig. 1 shows this situation schematically for a plane surface covered by a fluid layer.

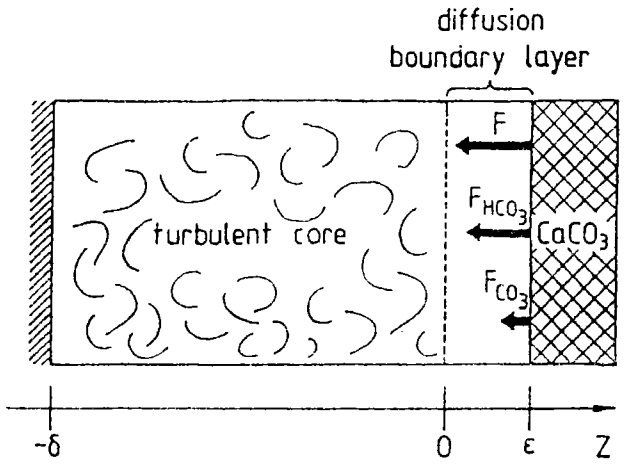

Fig.1. $CaCO_3$-CO_2-H_2O system with turbulent core and diffusion boundary layer ϵ ($\delta >> \epsilon$). $\delta+\epsilon$ represents the thickness of water layer in contact to the solid.

Inside the boundary layer mass flux (F) from the solid into the bulk is entirely determined by molecular diffusion. If no chemical reaction of the dissolved species occur the flux F is given by:

$$F=(D/\epsilon)(C_W-C_B) \qquad (1)$$

where C_W is the concentration at the solid and C_B that in the bulk and D is the coefficient of molecular diffusion. Eq.(1), however, provides no progress unless one knows the value of ϵ. This can be done by dissolution experiments where mass transport is entirely controlled by molecular diffusion as in the case of dissolution of gypsum ($CaSO_4 \cdot 2H_2O$). Under these conditions $C_W=C_B$ is equal the saturation concentration and C_B and F can be determined experimentally for a given situation (Opdyke et al., 1987).

Another way of estimating ϵ is the use of hydrodynamic semi-empirical correlations for a given hydrodynamic environment. A suitable expression for rectangular plates of length L employed in our field studies, is given by Skelland (1974):

$$\epsilon=2.703L^{0.2}(\upsilon/V)^{0.8} \qquad (2)$$

where υ is the kinematic viscosity and V the average flow velocity.

The influence of ϵ on the dissolution and precipitation of calcite, where chemical reactions i.e. slow conversion from $CO_2 \leftrightarrow HCO_3^-$ occur has been investigated in detail by Buhmann & Dreybrodt (1985a,b), taking into the account molecular diffusion across a diffusion boundary layer of thickness ϵ adjacent to the liquid-solid interface. Fig. 2 displays an example of their results on deposition rates from solutions supersaturated with respect to calcite under open system conditions and various CO_2 pressures as they are of interest in this

context. The different curves in Fig.2 have been calculated for various thicknesses ϵ of the diffusion boundary layer. The uppermost curves show the limiting situation of perfect turbulence and neglecting a boundary layer i.e. ϵ=0. With increasing ϵ the rates decrease significantly towards a threshold, which is reached at ϵ≈0.02cm. This shows, that depending on the flow velocities of the solution, deposition rates may change by about one order of magnitude, even though the chemical composition of the solution remains constant.

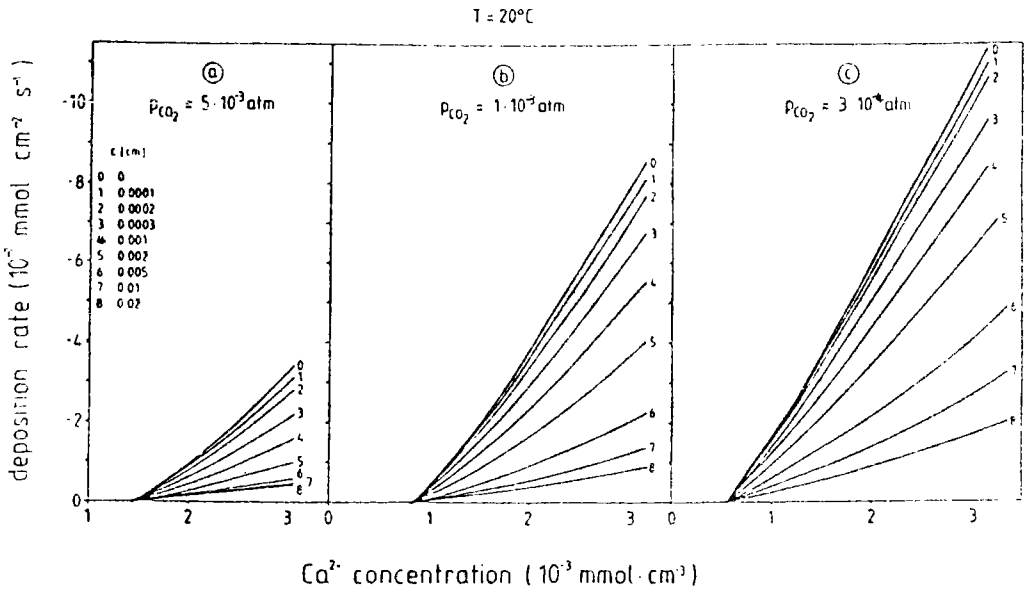

Fig.2. Deposition rates of calcite in an open system as a function of the Ca^{2+} concentration in the solution at different atmospheric CO_2 pressures. The *numbers* on the curves are related to the thickness ϵ of the boundary layer as listed in 2 (a). Thickness of the water layer: δ=1cm.

3.*Geomorphologic and Geological Setting of Huanglong*

Huanglong Ravine is located in the northwestern Plateau of Sichuan province at an altitude of roughly 3400m asl. Because of its overwhelming scenery with large tufa deposits it is a famous, natural attraction and, moreover, a typical site of modern alpine karst with a mean annual precipitation up to 759mm and an average annual air temperature of 1.1°C. Along a valley of 3.5km in length with an average width of 250m, very thick tufa has been deposited. A group of springs on an altitude of 3578m asl discharging about 50 $l \cdot s^{-1}$ represent the highest point while the lowest part is located on 3115m asl where calcite deposition ceases, when the Fu River crosses the valley. Because of the

yellow colour of the tufa and its morphologically resemblance to the shape of a dragon the location is named Huanglong (Yellow Dragon) Ravine. Fig.3 shows the location map including the sampling sites 9-1 downstream, where precicipitation experiments and investigations of the hydrochemistry have been performed. - Geologically, Huanglong is a region still active in neotectonism and bordered by steeply dipping faults and lithologically characterized by the occurrence of Silurian metamorphic rocks as well as calcareous sandstones, intercalated with silty slates of upperTriassic age. Among these series, at the source region of Huanglong Ravine and within an area of nearly 10 km^2 there is an outcrop of late Paleozoic limestone, mainly upper Devonian to Carbonifereous age (Zhu, 1991). The subsequent Quaternary glacial abrasion and their deposits, finally, have formed the present morphology. A geological profile of Huanglong region is given in Fig.4.

4.Methods and Materials

During two field campaigns in September 1991 and June 1992, experiments have been carried out in Huanglong Ravine to obtain detailed informations on both, hydrochemistry and calcite precipitation rates, because only few data have been published in the past related to the origin of the local tufa deposits (Chen, 1988; Zhu, 1989; 1990). In summary the aim of our investigations can be addressed to the following items:

- ***Analysis and Variations of Hydrochemistry***: Water temperature, pH and conductivity were measured in situ, while total hardness, Ca_T and total alkalinity (essential HCO_3^-) were measured immediately in the field after sampling, performing standard titration methods. In addition, sample volumes of 50ml each, passed through 0.45μm membrane filters were taken and preserved by addition of 1ml concentrated HNO_3. They were later analyzed for calcium, magnesium, sodium and sulphate by ICP, while cloride was determined by a standard titration method. From the data of the water analysis, PCO_2 and saturation state with respect to calcite (SI_C) have been calculated, applying the computer program SOLMINEQ.88 (Kharaka et al., 1988). From these chemical data and the PWP rate equation we were able to calculate the maximum rates, i.e. assuming $\epsilon=0$.
- ***Calcite Precipitation Rates***: Experiments have been conducted, employing pure marble tablets, cut into rectangular samples of about 3cmx3cmx0.3cm with an overall surface of 21.6cm^2. At each experimental site two samples were placed on top of a rimstone dam into quickly flowing water and close by inside a pool with still water, respectively. Samples were situated of about 3cm (rimstone dams) to 30cm (water pools) beneath the water surface, thus at any time the complete immersion of the tablets was guaranteed. The marble samples rested for a time period of about 4 days. Precipitation rates were determined by measuring weight increase of the samples.

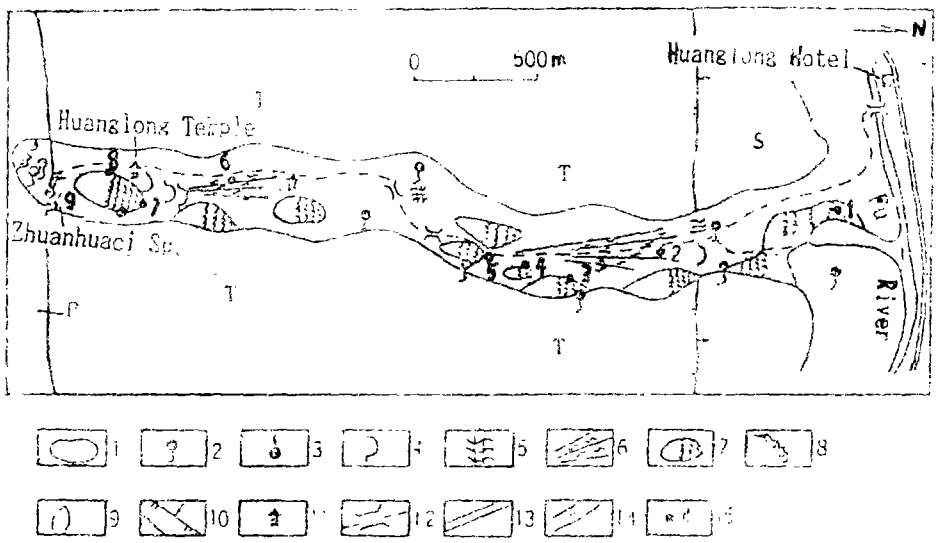

Fig.3. Map of Huanglong including the experimental sites 9-1

1--boundary of tufa scenery 2--descend spring 3--ascend spring 4--cave 5,6--tufa in different micro-shape 7--rimstones and pools 8--end moraine 9--Quaterny glacial deposits 10--fault 11--temple 12--tourism trail 13--highway 14--Fu River 15--experimental sites and number.

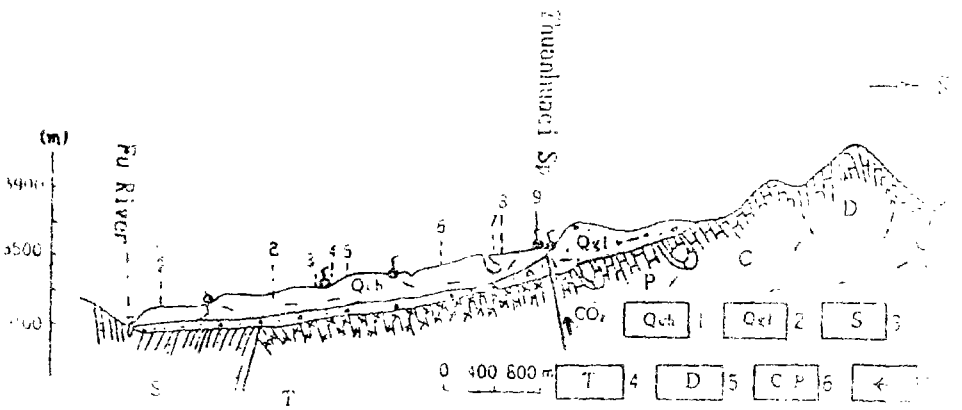

Fig.4. Geological profile of Huanglong area

1--Quaterny tufa 2--Quaterny glacial sand and gravel 3--Silurian slate intercalated with sandstone 4--Triassic sandstone and slate 5--Devonian slate intercalated with limestone 6--Carboniferous to Permian limestone 7--flow direction of groundwater.

- ***Boundary Layer Thickness*** ϵ ***and Flow Velocity:*** To estimate the thickness ϵ of the diffusion boundary layer two methods were employed:

(i) We determined the flux of Ca^{2+} from the gypsum samples which were of similar shape as the marble tablets and closely placed to the latter, by weight loss after immersion in the water for about 5 to 8 hours. The thickness ϵ was then calculated by Eq.(1).

(ii) the flow velocity of the stream was measured by applying a pitot tube. The velocity thus obtained, was used to determine ϵ from Eq.(2).

From the analyzed data, by use of the program SOLMINEQ.88, we calculated the concentrations of Ca^{2+}, Mg^{2+} and HCO_3^-, while from pH and temperature we have computed PCO_2 and SI with respect to calcite. The results are listed in Table 1 and are visualized in Fig.5 by downstream profiles of water temperature, pH, total hardness, HCO_3^-, PCO_2 and SI_C from sampling sites 9-1.

Table 1. Major chemical parameters from site 9-1 downstream for both field campaigns in September 91 and June 92.

site No.	field campaign	T_w (°C)	pH	SpC (μS)	Ca^{2+} (mol/l)	Mg^{2+} (mol/l)	HCO^{-3} (mol/l)	PCO_2 (atm)	SI calcite	Ca/Mg
	1991	6.0	6.44	999	$4.93 \cdot 10^{-3}$	$8.93 \cdot 10^{-4}$	$1.22 \cdot 10^{-2}$	0.23	-0.19	5.40
9										
	1992	6.3	6.41	1027	$5.05 \cdot 10^{-3}$	$8.21 \cdot 10^{-4}$	$1.27 \cdot 10^{-2}$	0.26	-0.20	5.96
	1991	5.1	8.04	870	$4.48 \cdot 10^{-3}$	$8.18 \cdot 10^{-4}$	$1.07 \cdot 10^{-2}$	$5.2 \cdot 10^{-3}$	1.30	5.44
8										
	1992	7.8	7.86	895	$4.37 \cdot 10^{-3}$	$7.51 \cdot 10^{-4}$	$1.08 \cdot 10^{-2}$	$7.9 \cdot 10^{-3}$	1.16	5.76
	1991	4.3	8.26	588	$3.21 \cdot 10^{-3}$	$6.21 \cdot 10^{-4}$	$6.77 \cdot 10^{-3}$	$2.0 \cdot 10^{-3}$	1.20	5.14
7										
	1992	4.9	8.13	431	$2.00 \cdot 10^{-3}$	$4.15 \cdot 10^{-4}$	$4.89 \cdot 10^{-3}$	$2.0 \cdot 10^{-3}$	0.77	4.80
	1991	3.6	8.36	461	$2.56 \cdot 10^{-3}$	$5.13 \cdot 10^{-4}$	$5.08 \cdot 10^{-3}$	$1.2 \cdot 10^{-3}$	1.09	4.98
6										
	1992	5.3	8.33	356	$1.63 \cdot 10^{-3}$	$3.57 \cdot 10^{-4}$	$4.36 \cdot 10^{-3}$	$1.1 \cdot 10^{-3}$	0.85	4.58
	1991	4.0	8.38	497	$2.60 \cdot 10^{-3}$	$6.10 \cdot 10^{-4}$	$5.53 \cdot 10^{-3}$	$1.3 \cdot 10^{-3}$	1.15	4.27
5										
	1992	5.7	8.44	413	$1.82 \cdot 10^{-3}$	$4.34 \cdot 10^{-4}$	$4.95 \cdot 10^{-3}$	$9.8 \cdot 10^{-4}$	1.06	4.19
	1991	3.3	8.45	482	$2.49 \cdot 10^{-3}$	$6.17 \cdot 10^{-4}$	$5.31 \cdot 10^{-3}$	$1.0 \cdot 10^{-3}$	1.18	4.04
4										
	1992	5.7	8.49	424	$1.90 \cdot 10^{-3}$	$4.34 \cdot 10^{-4}$	$4.80 \cdot 10^{-3}$	$9.5 \cdot 10^{-4}$	1.11	4.39
	1991	5.4	8.48	445	$2.31 \cdot 10^{-3}$	$6.22 \cdot 10^{-4}$	$4.82 \cdot 10^{-3}$	$8.7 \cdot 10^{-4}$	1.17	3.77
3										
	1992	5.6	8.41	401	$1.66 \cdot 10^{-3}$	$4.65 \cdot 10^{-4}$	$4.32 \cdot 10^{-3}$	$9.2 \cdot 10^{-4}$	0.93	3.56
	1991	5.3	8.35	414	$2.20 \cdot 10^{-3}$	$6.22 \cdot 10^{-4}$	$4.71 \cdot 10^{-3}$	$1.1 \cdot 10^{-3}$	1.11	3.54
2										
	1992	6.4	8.47	392	$1.56 \cdot 10^{-3}$	$4.72 \cdot 10^{-4}$	$4.72 \cdot 10^{-3}$	$8.8 \cdot 10^{-4}$	1.02	3.33
	1991	6.3	8.42	397	$2.09 \cdot 10^{-3}$	$6.10 \cdot 10^{-4}$	$4.49 \cdot 10^{-3}$	$9.3 \cdot 10^{-4}$	1.06	3.43
1										
	1992	7.0	8.43	339	$1.65 \cdot 10^{-3}$	$4.94 \cdot 10^{-4}$	$4.31 \cdot 10^{-3}$	$8.8 \cdot 10^{-4}$	1.06	3.43

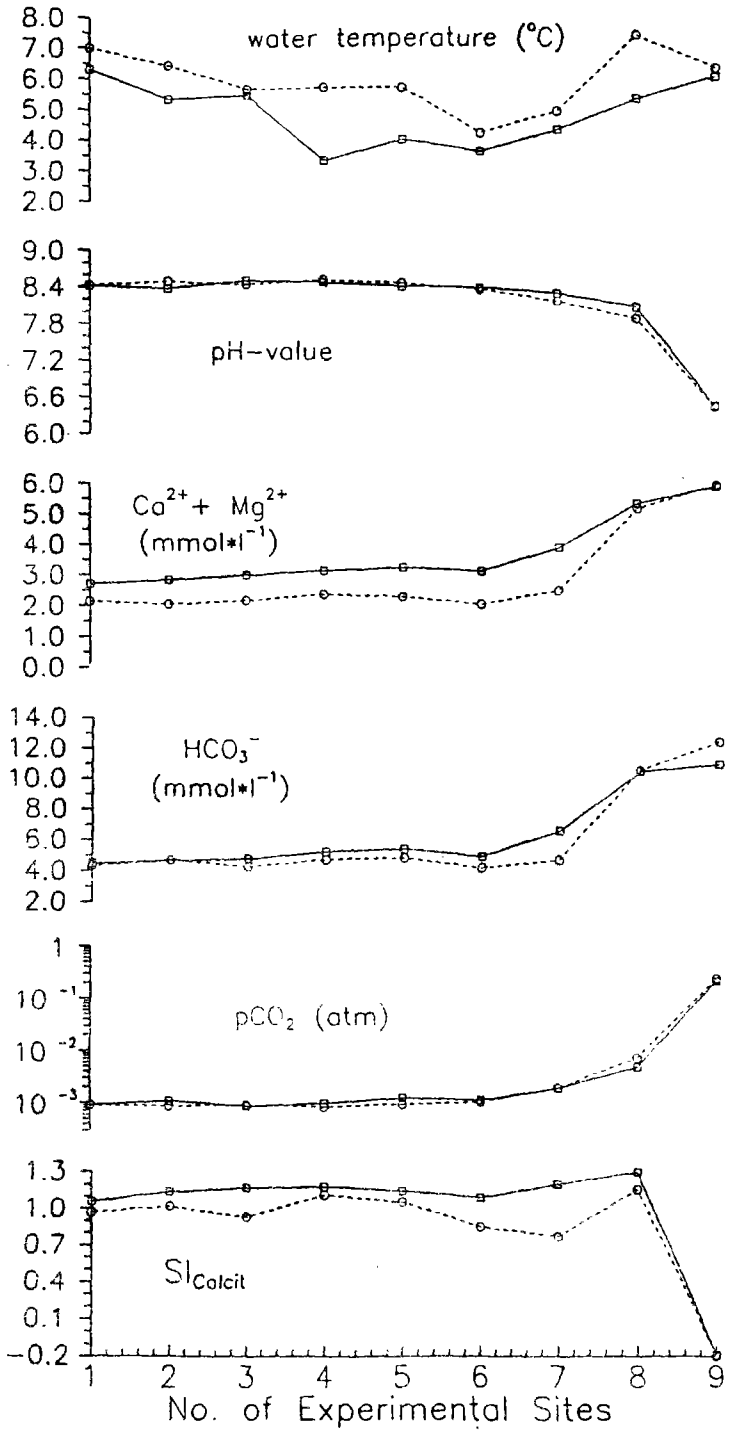

Fig.5. Profiles of important parameters illustrating the downstream evolution of water chemistry from the sites 9-1.

- Solid lines through open cubes: Results from September 91
- Dashed lines through open circles: Results from June 92.

Qualitatively, the observed patterns in water chemistry are similar for both investigations, although analyzed concentrations, e.g. Ca^{2+}+Mg^{2+} have been distinctly lowered during our last study in June 92. This becomes reasonable, because permanent heavy rain together with considerable supply of water from snowmelt diluted the stream water at sites 7-6. Between site 9 (spring water) and site 8 (about 200m downstream) a strong decrease in PCO_2 due to CO_2 outgassing is observed. In consequence, pH increases steeply also accompanied by a strong increase in SI_C causing heavy calcite precipitation at site 8, whereby the Ca^{2+} concentration drops remarkably. While along the stream course from site 6-1 pH, PCO_2 and SI_C display only minor variation the concentrations of Ca^{2+} and HCO_3^-, in contrast, decrease continuously by calcite precipitation. This is also mirrored by a steady decrease in the Ca^{2+}/Mg^{2+} ratio due to the removal of Ca^{2+}, while the concentrations of Mg^{2+} remain almost constant. The other species SO_4^{2-}, Na^+ and Cl^- show little variations, indicating no additional inputs of different waters.

Table 2 lists the measured precipitation rates in comparison with the rates, calculated by the rate law of Plummer, Wigley and Parkhurst from the chemical water data in Table 1. Furthermore, the values of the thicknesses ϵ of the laminar boundary layer are given as determined from weight loss by dissolution of gypsum tablets (Eq.1) and the results from measurements of the water velocities (Eq.2), respectively. The values of ϵ obtained from the pool studies are larger by a factor of 2-3 compared to those that have been obtained on rimstone dams at high flow velocities.

5. Results and Discussion

Figs. 6 and 7 present the precipitation rates measured during both campaigns in comparison with the maximum rates (ϵ=0), derived from the PWP-rate law. In each of the studies we observed that the profile of the PWP-rates is quite similar to those of the rates at the rimstone dams, which are significantly lower. The rates in the pools, furthermore, are lower by a factor of about 3 to 4 than those on the dams. This clearly demonstrates the influence of the hydrodynamic conditions on calcite precipitation rates, since the hydrochemistry at a given dam site and 30cm apart in the corresponding pool is identical. Thus the predictions of the theory by Dreybrodt & Buhmann (1991) are well confirmed under the conditions of a natural system.

In contrast to the first campaign in September 91, where we have been observed perceptible rates at sites 7-6, no deposition has been found during our last study in June 92. As mentioned above, the inspection of Table 2 shows that due to heavy rain and considerable recharge by snowmelt from the mountains, the SI_C has dropped down to 0.77 and 0.85, respectively, whereas in the first study it was 1.2 and 1.09. This observation shows that in natural systems obviously a threshold for calcite deposition exists for $SI_C \leq 0.85$. Below this value calcite deposition ceases. This observations are in good agreement

Table 2. Measured calcite deposition rates and thicknesses ϵ determined by gypsum field experiments and calculated from Eq.(2) for both campaigns.

site No	field campaign (year)	type of experimental location	dep. rates of calcite (cm/y)	ϵ gypsum (cm)	ϵ calculated (cm)	flow velocity (cm/s)	SI calcite	PCO_2 (atm)	PWP dep. rate (cm/y)
8	1991	rimstone dam	$4.7 \cdot 10^{-1}$	$5.1 \cdot 10^{-3}$	$1.4 \cdot 10^{-2}$	50	1.30	$5.2 \cdot 10^{-3}$	$6.1 \cdot 10^{-1}$
	1991	water pool	$1.3 \cdot 10^{-1}$	$2.0 \cdot 10^{-2}$					
	1992	rimstone dam	$2.9 \cdot 10^{-1}$	$7.0 \cdot 10^{-3}$	$1.1 \cdot 10^{-2}$	95	1.16	$7.9 \cdot 10^{-3}$	$5.1 \cdot 10^{-1}$
	1992	water pool	$7.4 \cdot 10^{-2}$	$1.7 \cdot 10^{-2}$					
4	1991	stream-bed	$2.5 \cdot 10^{-1}$	$3.9 \cdot 10^{-3}$	$1.2 \cdot 10^{-2}$	60	1.20	$2.0 \cdot 10^{-3}$	$5.5 \cdot 10^{-1}$
	1991	water-pool	$6.0 \cdot 10^{-2}$	$1.2 \cdot 10^{-2}$					
	1992	stream-bed	$< 1 \cdot 10^{-3}$	$5.9 \cdot 10^{-3}$	$8.7 \cdot 10^{-3}$	120	0.77	$2.0 \cdot 10^{-3}$	$2.1 \cdot 10^{-1}$
	1192	stream-bed	$< 1 \cdot 10^{-3}$	$5.6 \cdot 10^{-3}$					
6	1991	stream-bed	$1.4 \cdot 10^{-1}$	$2.8 \cdot 10^{-3}$	$7.0 \cdot 10^{-3}$	100	1.09	$1.2 \cdot 10^{-3}$	$1.5 \cdot 10^{-1}$
	1991	water-pool	$1.1 \cdot 10^{-2}$	$6.9 \cdot 10^{-3}$					
	1992	stream-bed	$< 1 \cdot 10^{-3}$	$5.2 \cdot 10^{-3}$	$5.3 \cdot 10^{-3}$	200	0.85	$1.1 \cdot 10^{-3}$	$2.1 \cdot 10^{-1}$
	1992	stream-bed	$< 1 \cdot 10^{-3}$	sample lost					
5	1991	stream-bed	$1.1 \cdot 10^{-1}$	$5.0 \cdot 10^{-3}$	$1.2 \cdot 10^{-2}$	60	1.15	$1.3 \cdot 10^{-3}$	$4.8 \cdot 10^{-1}$
	1991	water-pool	sample lost	$6.6 \cdot 10^{-3}$					
	1992	rimstone dam	$3.8 \cdot 10^{-2}$	$1.2 \cdot 10^{-2}$	$1.5 \cdot 10^{-2}$	71	1.06	$9.8 \cdot 10^{-4}$	$3.6 \cdot 10^{-1}$
	1992	water pool	sample lost	$2.2 \cdot 10^{-2}$					
1	1991	rimstone dam	sample lost	-	-	-	1.18	$1.0 \cdot 10^{-3}$	$5.2 \cdot 10^{-1}$
	1991	water pool	sample lost	-					
	1992	rimstone dam	$6.6 \cdot 10^{-2}$	$7.7 \cdot 10^{-3}$	$1.7 \cdot 10^{-2}$	60	1.11	$8.5 \cdot 10^{-4}$	$4.1 \cdot 10^{-1}$
	1992	water pool	$2.6 \cdot 10^{-2}$	$2.4 \cdot 10^{-2}$					
3	1991	rimstone dam	$1.1 \cdot 10^{-1}$	$5.1 \cdot 10^{-3}$	$1.8 \cdot 10^{-2}$	40	1.17	$8.7 \cdot 10^{-4}$	$5.2 \cdot 10^{-1}$
	1991	water pool	$4.3 \cdot 10^{-2}$	$2.2 \cdot 10^{-2}$					
	1992	rimstone dam	$5.5 \cdot 10^{-2}$	$7.7 \cdot 10^{-3}$	$1.3 \cdot 10^{-2}$	78	0.93	$9.2 \cdot 10^{-4}$	$2.9 \cdot 10^{-1}$
	1992	water pool	$1.6 \cdot 10^{-2}$	$2.4 \cdot 10^{-2}$					
7	1991	stream-bed	$1.4 \cdot 10^{-1}$	$2.3 \cdot 10^{-3}$	$4.7 \cdot 10^{-3}$	150	1.14	$1.1 \cdot 10^{-3}$	$3.9 \cdot 10^{-1}$
	1991	water pool	sample lost	-					
	1992	stream bed	$6.3 \cdot 10^{-2}$	$9.0 \cdot 10^{-3}$	$1.1 \cdot 10^{-2}$	97	1.02	$8.8 \cdot 10^{-4}$	$3.1 \cdot 10^{-1}$
	1992	stream-bed	$4.9 \cdot 10^{-2}$	$1.0 \cdot 10^{-2}$					
2	1991	rimstone dam	$1.9 \cdot 10^{-1}$	$3.2 \cdot 10^{-3}$	$8.8 \cdot 10^{-3}$	80	1.06	$9.3 \cdot 10^{-4}$	$4.1 \cdot 10^{-1}$
	1991	water pool	$5.6 \cdot 10^{-2}$	$1.2 \cdot 10^{-2}$					
	1992	rimstone dam	$1.2 \cdot 10^{-2}$	$3.6 \cdot 10^{-3}$	$8.7 \cdot 10^{-3}$	120	0.97	$8.8 \cdot 10^{-4}$	$3.1 \cdot 10^{-1}$
	1992	water pool	$5.4 \cdot 10^{-3}$	$3.6 \cdot 10^{-2}$					

with results from field and laboratory experiments and with data of other researchers, who observed that calcite deposition was missing in waters with $SI_C < 1.0$ (Dreybrodt, 1988). The main advantage in our studies is that we observe both situations, i.e. $SI_C < 1.0$ and $SI_C > 1.0$ at the same site and for nearly the same type of water.

We now will compare the observed to the theoretically predicted rates, which are depictable from Fig.2 for different CO_2-pressures of $5 \cdot 10^{-3}$ atm and $1 \cdot 10^{-3}$ atm, respectively. This is performed by linear extrapolation of the curves, if necessary. Precipitation rates measured in the pools (still water) are determined by boundary layer thicknesses of about 10^{-2}cm, which all correspond to the lowest curves in Fig.2 and are in the order of 10^{-2}cm$\cdot$y^{-1}. They agree with the observed data, within a factor of 2. For values of $\epsilon \approx 5 \cdot 10^{-3}$cm from Fig.2 we

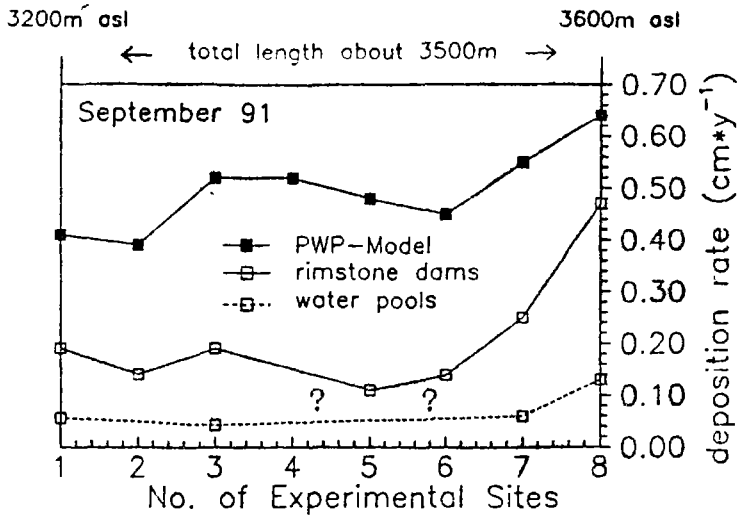

Fig.6. Calcite deposition rates in dependence of various hydrodynamic conditions from field campaign in September 91.

- Solid lines through full cubes: Maximum rates predicted by the PWP-rate law, calculated from hydrochemical data on Table 1.
- Solid lines through open cubes: Measured calcite deposition rates at the rimstone dams (fast flow).
- Dashed lines through open cubes: Measured calcite deposition rates inside the water pools (slow flow). - Lost samples are indicated by (??).

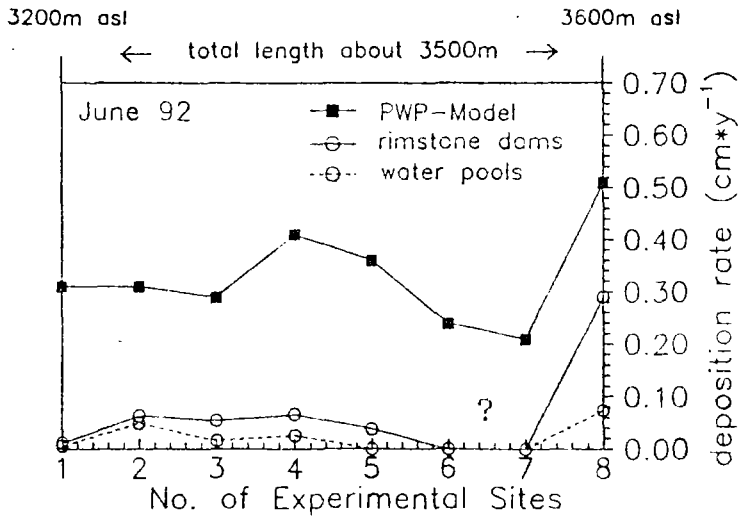

Fig.7 Calcite deposition rates in dependence of various hydrodynamic conditions from field campaign in June 92.

- Solid lines through full circles: Maximum rates predicted by the PWP-rate law calculated from hydrochemical data on Table 1.
- Solid lines through open circles: Measured calcite deposition rates at the rimstone dams (fast flow).
- Dashed lines through open circles: Measured calcite deposition rates inside the water pools (slow flow). - Precipitation rates < $1 \cdot 10^{-3}$ cm·y-1 are indicated by (?).

final rates, which are lower than the corresponding maximum rates by a factor of about 0.2 to 0.3. The values of ϵ estimated from the stream velocity by Eq.(2) are in the order of 10^{-2}cm. This indicates that this method may not be very appropriate. The rates at site 8 are especially high, much higher than predicted by the theory. This might indicate that the estimation of ϵ by dissolution of gypsum tablets gives too high values for ϵ. Probably hydrodynamic similarity of the gypsum tablets was not obtained. For future work we will use alabaster tablets, instead of crystalin "Marienglas". These alabaster tablets will be cut exactly like the marble tablets and also will be polished the same way.

In summary we conclude, that the profiles of the measured precipitation rates resemble very much that of the rates predicted by the PWP-rate law, calculated from the data of the water analysis. Thus the rates of Huanglong Ravine can be estimated from the PWP-rates by multiplying by a factor of 0.2. This result is similar to what we have obtained at the Westerhofbach (Dreybrodt et al., 1992). The stream system of Huanglong, however, exhibits much higher calcite precipitation rates. It represents an anthropologically unpolluted system with a water chemistry that is determined almost entirely by the Ca-HCO_3 type. Therefore it is ideally suited to carry out further experiments, related to elucidate the influence of different hydrodynamic conditions on calcite precipitation. This can be performed by use of samples with various geometric shapes, which are planned for future studies. Moreover, it is a suitable field for studies in $\delta^{13}C$ isotopic compositions of dissolved and precipitated carbonate or in $\delta^{18}O$ isotopes of calcite. Figs. 8 and 9 give a first set of data from our last study in June 92. The $\delta^{13}C$ values of the calcite samples are in close agreement with those analyzed by Chen (1988) at site 8 who found $\delta^{13}C$ values within +4.25 to +4.81 ($^{o}/_{oo}$, PDB). Additionally, we sampled gas by catching ascending bubbles directly inside the spring pits at site 9. The analysis shows $\delta^{13}C$ of -6.79 ($^{o}/_{oo}$, PDB), indicating a juvenile origin of the CO_2. This is in good accordance with the above-mentioned neotectonically activities in this region, still present today.

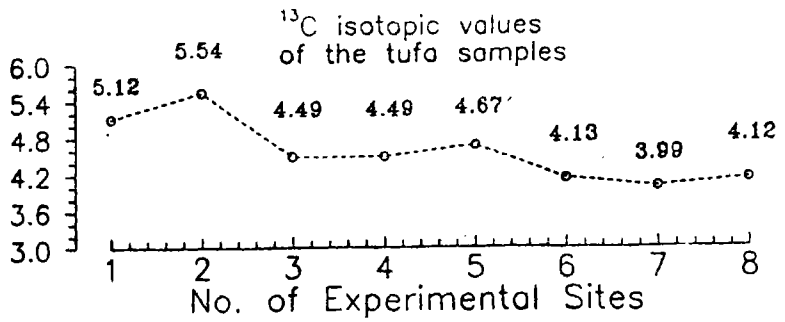

Fig.8. Analyzed $\delta^{13}C$ isotopic values of the sampled tufas from sites 8-1 downstream from field campaign in June 92.

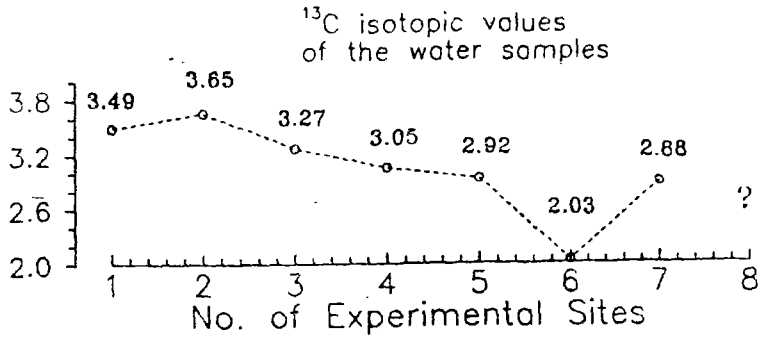

Fig.9. Analyzed $\delta^{13}C$ isotopic values of the water samples from sites 8-1 downstream collected during field campaign in June 92. Lost sample is indicated by (?).

Together with newly planned investigations - including other topics for research activities - we hope that our young Chinese-German cooperation will be continued so sucessfully as it has started. The present aim is, doubtlessly, to reveal the origin and/or morphogentic aspects that have favoured such extraordinary tufa deposits in space and time. It has started roughly 8000 years before present and hopefully will grow on.

Acknowledgements

We are gratefully acknowledge financial support for this study granted to us by the German Research Council (DFG) and support of the National Natural Science Foundation of China. We are also indebted to Mr. He Dianbin and Mr. He Siyi for their valuable assistance during our field work as well as to the National Park Police of Huanglong Ravine Resort for supporting our activities.

References

Buhmann, D. & Dreybrodt, W. (1985a): The kinetics of calcite dissolution and precipitation in geologically relevant situations of karst areas. 1. Open system - Chem. Geol. **48**. 189-211.

Buhmann, D. & Dreybrodt, W. (1985b): The kinetics of calcite dissolution and precipitation in geologically relevant situations of karst areas. 2. Closed system. - Chem. Geol. **53**: 109-124.

Buhmann, D. & Dreybrodt, W. (1987): Calcite dissolution kinetics in the system H_2O-CO_2-$CaCO_3$ with participation of foreign ions. - Chem. Geol. **64**: 89-102.

Chen, X. (1988): A study on Isotopes of Karst Water and Travertine Deposits at the Huanglong Scenic Spot. - Carsologica Sinica, Vol.7, No.3. 209-217

Dreybrodt, W. (1988): Processes in Karst Systems. - Physics, Chemistry and Geology. Springer, Berlin, 288pp.

Dreybrodt, W. & Buhmann, D. (1991): A mass transfer model for dissolution and precipitation of calcite from solutions in turbulent motion. Chem. Geol. **90**. 107-122.

Dreybrodt, W., Buhmann, D., Michaelis, J. & Usdowski, E. (1992): Geochemically controlled calcite precipitation by CO_2 outgassing: Field measurements of precipitation rates in comparison to theoretical predictions. Chem. Geol. **97**: 285-294.

Herman, J.S. & Lorah, M.M. (1986): Groundwater geochemistry in Warm River Cave, Virginia. - Natl. Soc. Speleol. Bull. **48**: 54-61.

Herman, J.S. & Lorah, M.M. (1987): CO_2 outgassing and calcite precipitation in Falling Spring Creek, Virginia, USA. - Chem. Geol. **62**: 251-262.

Herman, J.S. & Lorah, M.M. (1988): Calcite precipitation rates in the field. Measurements and prediction for the travertine-depositing stream. - Geochim. Cosmochim. Acta **52**: 2347-2355.

Jacobson, R.L. & Usdowski, E. (1975): Geochemical Controls on a Calcite Precipitating Spring. - Contrib. Mineral. Petrol. **51**: 65-74.

Plummer, L.N., Parkaka, Y.K., Gunter, W.D., Aggarwaal P.K. Perkins, E.H. & Debraal, J.D. (1988): SOLMINEQ.88 - A computer program for geochemical modelling of water-rock interactions. U.S. Geol. Surv., Water-Resour. Invest. Rep., No. 88-4227: 207pp.

Michaelis, J., Usdowski, E. & Menschel, G. (1984): Kinetische Faktoren der $CaCO_3$-Abscheidung und der Fraktionierung von ^{12}C und ^{13}C. - Z. Wasser Abwasser-Forsch. **17**: 31-36.

Sparklyke, B.N., Gust, D. & Ledwell, J.R. (1987): Mass transfer from smooth alabaster surfaces in turbulent flows. - Geophys. Res. Lett. **14**: 1131-1134.

Plummer, L.N., Wigley, T.M.L. & Parkhurst, D.L. (1978): The kinetics of calcite dissolution in CO_2-water systems at 5°C to 60°C and 0.0 to 1.0 atm CO_2. - Am. J. Sci **278**: 179-216.

Plummer, L.N., Parkhurst, D.L. & Wigley, T.M.L. (1979): Critical review of calcite dissolution and precipitation. In: E.A. Jenne (Editor), Chemical Modelling in Aqueous Systems. Am. Chem. Soc. Symp. Ser., **93**: 537-573.

Usdowski, E., Hoefs, J. & Menschel, G. (1979): Relationship between ^{13}C and ^{18}O Fractionation and Changes in Major Element Composition in a recent Calcite-Depositing Spring. - A Model of Chemical Variations with Inorganic $CaCO_3$ Precipitation. Earth Planet. Sci. Lett. **42**: 267-276.

Skelland, A.H.P. (1974): Diffusional mass transport. - Wiley, New York, N.Y., 510pp.

Suarez, D.L. (1983): Calcite supersaturation and precipitation kinetics in the lower Colorado River, All American Canal and East Highland Canal. - Water Resour. Res. **19**: 653-661.

Troester, W.T. & White, W.B. (1986): Geochemical investigations of three tropical karst drainage basins in Puerto Rico. - Ground Water **24**: 475-482.

Zhu, Y. (1991): Alpine Karst in Huanglong Ravine. - The Chinese National Working Group of IGCP 299; The Institute of Karst Geology, Guilin, China: 33-37.

Zhu, X. (1989): Basic Characteristics of Karst Area in Minshan Mt., West Sichuan. - Carsologica Sinica, Vol.7, No 4: 253-260.

Zhu, X. (1990): Deposition of Travertines in Karst Area of Minshan Mt. - Carsologica Sinica, Vol.9, No.3: 250-264